Energy spectrum of tau leptons induced by the high energy Earth-skimming neutrinos

Jie-Jun Tseng,[1,*] Tsung-Wen Yeh,[2,†] H. Athar,[2,3,‡] M. A. Huang,[4,§] Fei-Fain Lee,[2,‖] and Guey-Lin Lin[2,¶]
[1]*Institute of Physics, Academia Sinica, Taipei 115, Taiwan*
[2]*Institute of Physics, National Chiao-Tung University, Hsinchu 300, Taiwan*
[3]*Physics Division, National Center for Theoretical Sciences, Hsinchu 300, Taiwan*
[4]*Department of Physics, National Taiwan University, Taipei 10617, Taiwan*
(Received 28 May 2003; published 26 September 2003)

We present a semianalytic calculation of the tau-lepton flux emerging from the Earth induced by incident high energy neutrinos interacting inside the Earth for $10^5 \leqslant E_\nu/\mathrm{GeV} \leqslant 10^{10}$. We obtain results for the energy dependence of the tau-lepton flux coming from the Earth-skimming neutrinos, because of the neutrino-nucleon charged-current scattering as well as the resonant $\bar{\nu}_e e^-$ scattering. We illustrate our results for several anticipated high energy astrophysical neutrino sources such as the active galactic nuclei, the gamma-ray bursts, and the Greisen-Zatsepin-Kuzmin neutrino fluxes. The tau-lepton fluxes resulting from rock-skimming and ocean-skimming neutrinos are compared. Such comparisons can render useful information about the spectral indices of incident neutrino fluxes.

DOI: 10.1103/PhysRevD.68.063003 PACS number(s): 95.85.Ry, 14.60.Fg, 14.60.Pq, 95.55.Vj

I. INTRODUCTION

The detection of high energy neutrinos ($E_\nu > 10^5$ GeV) is crucial to identify the extreme energy sources in the Universe and possibly to unveil the puzzle of cosmic rays with energy above the Greisen-Zatsepin-Kuzmin (GZK) cutoff [1]. These proposed scientific aims are well beyond the scope of conventional high energy gamma-ray astronomy. Because of the expected small flux of the high energy neutrinos, large scale detectors ($\geqslant 1$ km^2) seem to be needed to obtain the first evidence.

There are two different strategies to detect the footprints of high energy neutrinos. The first strategy is implemented by installing detectors in a large volume of ice or water where most of the scatterings between the candidate neutrinos and nucleons occur essentially inside the detector, whereas the second strategy aims at detecting the air showers caused by the charged leptons produced by the neutrino-nucleon scatterings taking place inside the Earth or in the air, far away from the instrumented volume of the detector. The latter strategy thus includes the possibility of detection of quasihorizontal incident neutrinos, which are also referred to as Earth-skimming neutrinos. These neutrinos are considered to interact below the horizon of an Earth based surface detector.

The second strategy has been proposed only recently [2]. The Pierre Auger observatory group has simulated the anticipated detection of the air showers from the decays of τ leptons [3]. The tau air shower event rates resulting from the Earth-skimming tau neutrinos for different high energy neutrino telescopes are given in [4]. A Monte Carlo study of the tau air shower event rate was also reported not long ago [5]. We note that Ref. [4] does not consider the tau-lepton energy distribution in the ν_τ-nucleon scattering, and only the incident tau neutrinos with energies greater than 10^8 GeV are considered. For Ref. [5], we note that only the sum of tau air shower event rates arising from different directions is given. Hence some of the events may be due to tau-leptons or neutrinos traversing a large distance. As a result, it is not possible to identify the source of the tau-neutrino flux even with the observation of the tau-lepton induced air shower.

In this work, we shall focus on high energy Earth-skimming neutrinos and shall calculate the energy spectrum of their induced tau leptons, taking into account the *inelasticity* of neutrino-nucleon scatterings and the tau-lepton *energy loss* in detail. Our work differs from Ref. [5] in our emphasis on the Earth-skimming neutrinos. We shall present our results in the form of outgoing tau-lepton spectra for different distances inside the rock, instead of integrating the energy spectra. As will be demonstrated, such spectra are insensitive to the distances traversed by the Earth-skimming ν_τ and τ. They are essentially determined by the tau-lepton range. Because of this characteristic feature, our results are useful for setting up simulations with specifically chosen air shower content detection strategy, such as detection of the Cherenkov radiation or the air fluorescence. Our results are also beneficial for the coherent Cherenkov radio emission measurement detectors such as the Radio Ice Cherenkov Experiment (RICE) [6] and the upcoming Antarctic Impulsive Transient Array (ANITA) [7].

We start with our semianalytic description in Sec. II. The transport equations governing the evolutions of neutrino and tau-lepton fluxes will be derived. Using these, we then calculate the tau-lepton flux resulting from the resonant $\bar{\nu}_e e^- \rightarrow W^- \rightarrow \bar{\nu}_\tau \tau^-$ scattering. In Sec. III, we summarize our main results, namely, the tau-lepton energy spectra due to neutrino-nucleon scatterings. The implications of our results will be discussed here also. In particular, we shall point out

*Email address: gen@phys.sinica.edu.tw
†Email address: twyeh@cc.nctu.edu.tw
‡Email address: athar@phys.cts.nthu.edu.tw
§Present address: National United University, Miaoli 360, Taiwan. Email address: huangmh@phys.ntu.edu.tw
‖Email address: u8727515@cc.nctu.edu.tw
¶Email address: glin@cc.nctu.edu.tw

that the ratio of tau-lepton flux induced by rock-skimming neutrinos to that induced by ocean-skimming neutrinos is sensitive to the spectral index of the incident tau-neutrino flux. In Sec. IV, we discuss some prospects for possible future observations of the associated radiation from these tau leptons.

II. TAU-LEPTON ENERGY SPECTRUM

Let us begin with the transport equations for tau neutrinos and tau leptons. Considering only the neutrino-nucleon scatterings, we have

$$\frac{\partial F_{\nu_\tau}(E,X)}{\partial X} = -\frac{F_{\nu_\tau}(E,X)}{\lambda_{\nu_\tau}(E)} + n_N \sum_{i=1}^{3} \int_{y^i_{\min}}^{y^i_{\max}} \frac{dy}{1-y} \times F_i(E_y,X) \frac{d\sigma^i_\nu}{dy}(y,E_y) \tag{1}$$

and

$$\frac{\partial F_\tau(E,X)}{\partial X} = -\frac{F_\tau(E,X)}{\lambda^{\rm CC}_\tau(E)} - \frac{F_\tau(E,X)}{\rho d_\tau(E)} + \frac{\partial\{[\alpha(E)+\beta(E)E]F_\tau(E,X)\}}{\partial E} + n_N \int_{y_{\min}}^{y_{\max}} \frac{dy}{1-y} F_{\nu_\tau}(E_y,X) \frac{d\sigma_{\nu_\tau N\to\tau Y}}{dy}(y,E_y), \tag{2}$$

where n_N is the number of target nucleons per unit medium mass, and ρ is the mass density of the medium. The $\sigma^{1,2,3}_\nu$ are defined as $\sigma(\nu_\tau+N\to\nu_\tau+Y)$, $\Gamma(\tau\to\nu_\tau+Y)/c\rho n_N$, and $\sigma(\tau+N\to\nu_\tau+Y)$, respectively. The quantity X represents the slant depth traversed by the particles, i.e., the amount of medium per unit area traversed by the particle (and thus in units of g/cm^2). λ_ν, d_τ, and $\lambda^{\rm CC}_\tau$ represent the ν_τ interaction thickness, the tau-lepton decay length, and the tau-lepton charged-current interaction thickness, respectively, with, say, $\lambda_\nu^{-1}=n_N\sigma_{\nu N}$ and $d_\tau=c\tau_\tau E/m_\tau$. E_y is equal to $E/(1-y)$, where y is the inelasticity of neutrino-nucleon scatterings, such that the initial- and final-state particle energies in the differential cross sections $d\sigma^i_\nu(y,E_y)/dy$ and $d\sigma_{\nu_\tau N\to\tau Y}(y,E_y)/dy$ are $E/(1-y)$ and E, respectively. The limits for y, $y^i_{\min}$, and $y^i_{\max}$ depend on the kinematics of each process. Finally, the energy-loss coefficients $\alpha(E)$ and $\beta(E)$ are defined by $-dE/dX=\alpha(E)+\beta(E)E$ with E being the tau-lepton energy. An equation similar to Eq. (2) in the context of atmospheric muons was found in Ref. [8].

As mentioned before, Eqs. (1) and (2) take into account only neutrino-nucleon scatterings. It is of interest to calculate the tau-lepton fluxes produced by the Glashow resonance [9,10], namely, via $\bar{\nu}_e e^-\to W\to\bar{\nu}_\tau\tau^-$, also. The transport equation for $\bar{\nu}_e$ then reads

$$\frac{\partial F^-_{\bar{\nu}_e}(E,X)}{\partial X} = -\frac{F^-_{\bar{\nu}_e}(E,X)}{\lambda_{\bar{\nu}_e}(E)} + n_N \int_{y_{\min}}^{y_{\max}} \frac{dy}{1-y} \times F^-_{\bar{\nu}_e}(E_y,X) \frac{d\sigma^-_{\bar{\nu}_e N\to\bar{\nu}_e Y}}{dy}(y,E_y). \tag{3}$$

Similarly, the corresponding equation for the tau-lepton flux is given by

$$\frac{\partial F_\tau(E,X)}{\partial X} = -\frac{F_\tau(E,X)}{\lambda^{\rm CC}_\tau(E)} - \frac{F_\tau(E,X)}{\rho d_\tau(E)} + n_e \int_{y_{\min}}^{y_{\max}} \frac{dy}{1-y} F^-_{\bar{\nu}_e}(E_y,X) \frac{d\sigma^-_{\bar{\nu}_e e^-\to\bar{\nu}_\tau\tau^-}}{dy}(y,E_y), \tag{4}$$

where n_e is the number of target electrons per unit medium mass.

Before solving the above coupled transport equations, it is essential to know the energy-loss coefficients $\alpha(E)$ and $\beta(E)$. As pointed out before [11], the coefficient $\alpha(E)$ is due to the energy loss by ionization [12], while $\beta(E)$ is contributed by the bremsstrahlung [13], the e^+e^- pair production [14], and the photonuclear processes [11,15]. It is understood that the contribution by $\alpha(E)$ becomes unimportant for $E \geqslant 10^5$ GeV. The coefficient $\beta(E)$ can be parametrized as $\beta(E)=[1.6+6(E/10^9\ {\rm GeV})^{0.2}]\times 10^{-7}\ {\rm g}^{-1}\,{\rm cm}^2$ in standard rock for $10^5\leqslant E/{\rm GeV}\leqslant 10^{12}$.

It is of interest to check the tau-lepton range given by our semianalytic approach. To do this, we rewrite Eq. (2) by dropping the neutrino term, i.e.,

$$\frac{\partial F_\tau(E,X)}{\partial X} = -\frac{F_\tau(E,X)}{\lambda^{\rm CC}_\tau(E)} - \frac{F_\tau(E,X)}{\rho d_\tau(E)} + \frac{\partial[\gamma(E)F_\tau(E,X)]}{\partial E}, \tag{5}$$

with $\gamma(E)\equiv\alpha(E)+\beta(E)E$. One can easily solve it for $F_\tau(E,X)$:

$$F_\tau(E,X)=F_\tau(\bar{E},0)\exp\left[\int_0^X dT\left(\gamma'(\bar{E}) - \frac{1}{\rho d_\tau(\bar{E})} - \frac{1}{\lambda^{\rm CC}_\tau(\bar{E})}\right)\right], \tag{6}$$

where $\bar{E}\equiv\bar{E}(X;E)$ with $d\bar{E}/dX=\gamma(\bar{E})$ and $\bar{E}(0;E)=E$. To calculate the tau-lepton range, we substitute $F_\tau(E,0)=\delta(E-E_0)$. The survival probability $P(E_0,X)$ for a tau lepton with an initial energy E_0 at $X=0$ is

$$P(E_0,X)=\frac{\gamma(\tilde{E}_0)}{\gamma(E_0)}\exp\left[\int_0^X dT\left(\gamma'(\tilde{E}_0) - \frac{1}{\rho d_\tau(\tilde{E}_0)} - \frac{1}{\lambda^{\rm CC}_\tau(\tilde{E}_0)}\right)\right], \tag{7}$$

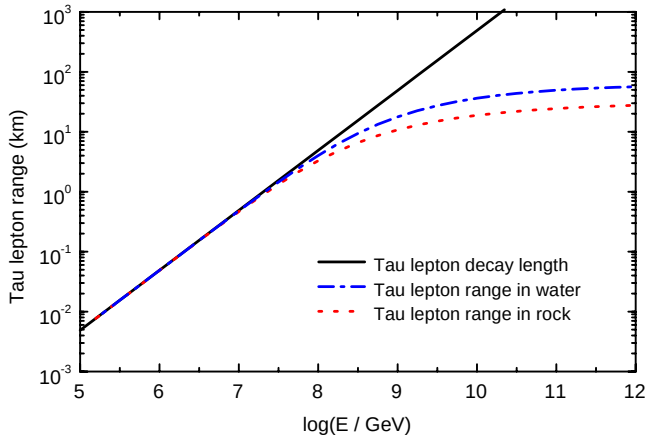

FIG. 1. The tau-lepton range in rock and in water using Eq. (8) and the tau-lepton decay length d_τ in km as a function of tau-lepton energy in GeV.

where $\tilde{E}_0 \equiv \tilde{E}(X;E_0)$ with $d\tilde{E}_0/dX = -\gamma(\tilde{E}_0)$ and $\tilde{E}_0(0;E_0)=E_0$. The tau-lepton range is simply

$$R_\tau(E_0) = \int_0^\infty dX P(E_0,X). \tag{8}$$

For $E_0 = 10^9$ GeV, we find that $R_\tau = 10.8$ km in standard rock ($Z=11$, $A=22$) while $R_\tau = 5.0$ km in iron. Both values are in good agreement with those obtained by Monte Carlo calculations [11]. To compare the tau-lepton ranges, we have followed the convention in Ref. [11] by requiring the final tau-lepton energy $\tilde{E}(X;E_0)$ to be greater than 50 GeV.

It is to be noted that we obtain R_τ by using the *continuous* tau-lepton energy-loss approach, rather than the stochastic approach adopted in Ref. [11]. In the muon case, the continuous approach to the muon energy loss is known to overestimate the muon range [16]. Such an overestimate is not significant in the tau-lepton case, because of the decay term in Eq. (7). In fact, tau-lepton decay term dictates the tau range in the rock until $E_\tau \geqslant 10^7$ GeV. Even for $E_\tau > 10^7$ GeV, the tau-lepton range is still not entirely determined by the tau-lepton energy loss. Hence different treatments on the tau-lepton energy loss do not lead to large differences in the tau-lepton range, in contrast to the case for the muon range. Our results for the tau-lepton range up to 10^{12} GeV are plotted in Fig. 1. This is an extension of the result in Ref. [11], where the tau-lepton range is calculated only up to 10^9 GeV. Our extension is seen explicitly in the addition of a charged-current scattering term on the right-hand side (RHS) of Eq. (5). This term is necessary because $1/\lambda_\tau^{CC}$ becomes comparable to $1/\rho d_\tau$ in rock for $E \geqslant 10^{10}$ GeV; whereas one does not need to include the contribution by the tau-lepton neutral-current scattering, since such a contribution cannot compete with the last term in Eq. (5) until $E \geqslant 10^{16}$ GeV [11]. We remark that our extended results for R_τ are subject to the uncertainties of the neutrino-nucleon scattering cross section at high energies. We use the CTEQ6 parton distribution functions [17] in this work, and at the high energy (the small x region, namely, for $x < 10^{-6}$), we fit these parton distribution functions into the form proportional to $x^{-1.3}$ as a guide.

Having checked the tau-lepton range, we now proceed to calculate the tau-lepton flux. It is instructive to begin with the simple case: the $\bar{\nu}_e e^-$ resonant scattering. It is well known that [9,10]

$$\sigma(\bar{\nu}_e e^- \to W^- \to \bar{\nu}_\tau \tau^-) = \frac{G_F^2 m_W^4}{3\pi} \cdot \frac{s}{(s-m_W^2)^2 + m_W^2 \Gamma_W^2}, \tag{9}$$

with $s = 2m_e E_{\bar{\nu}_e}$ and $1/\sigma \cdot d\sigma/dz = 3(1-z)^2$, where $z = E_\tau / E_{\bar{\nu}_e}$. We shall focus on only those $\bar{\nu}_e$'s for which $E_{\bar{\nu}_e}$ satisfies the resonance condition, i.e., $E_{\bar{\nu}_e} \approx E_R \equiv m_W^2/2m_e$. It is clear from Eq. (4) that $F_\tau(E,X)$ depends only on $F_{\bar{\nu}_e}(E_R,X)$, because of the narrow peak nature of $\bar{\nu}_e e^-$ scattering cross section. One also expects that $F_\tau(E,X)$ is significant only for E around the resonance energy E_R. In this energy region, one may neglect the first term on the RHS of Eq. (4) in comparison with the second term. In the narrow width approximation, the last term in Eq. (4) can be recast into $\frac{1}{3}(1-E/E_R)^2(\pi\Gamma_W/L_R m_W) F_{\bar{\nu}_e}(E_R,X)$, where Γ_W is the width of the W boson while L_R is the interaction thickness of the resonant $\bar{\nu}_e e^- \to W^-$ scattering (see Appendix A for details). The tau-lepton flux can be readily obtained once $F_{\bar{\nu}_e}(E_R,X)$ is given. We observe that the regeneration term in Eq. (3) (second term on the RHS) can be neglected as it is necessarily off the W boson peak. Hence, we easily obtain $F_{\bar{\nu}_e}(E_R,X) = \exp(-X/L_R) F_{\bar{\nu}_e}(E_R,0)$. Substituting this expression into Eq. (4), we obtain

$$\frac{F_\tau(E,X)}{F_{\bar{\nu}_e}(E_R,0)} = 3.3\times 10^{-4} \times \left(\frac{E}{E_R}\right) \times \left(1-\frac{E}{E_R}\right)^2 \times \exp\left(-\frac{X}{L_R}\right) \tag{10}$$

in the limit $X \gg \rho d_\tau$. The prefactor 3.3×10^{-4} is obtained by assuming a standard-rock medium. In water it becomes 1.4×10^{-4}. It is to be noted that $E < E_R$ in the above equation. We shall see later that the contribution to $F_\tau(E,X)$ by the W resonance is negligible compared to that by the ν_τ-N scattering.

Let us now turn to the case of tau-lepton production by ν_τ-N charged-current scattering. The tau-lepton flux can be calculated from Eqs. (1) and (2) once the incoming ν_τ flux is given. The ν_τ flux can be obtained by the following ansatz [18]:

$$F_{\nu_\tau}(E,X) = F_{\nu_\tau}(E,0) \exp\left(-\frac{X}{\Lambda_\nu(E,X)}\right), \tag{11}$$

where $\Lambda_\nu(E,X) = \lambda_\nu(E)/[1-Z_\nu(E,X)]$, with the factor $Z_\nu(E,X)$ arising from the regeneration effect of the ν_τ flux. On the other hand, the tau-lepton flux is given by

$$F_\tau(E,X)=\int_0^X dT G_\nu(\bar{E},T)\exp\left[\int_T^X dT'\left(\gamma'(\bar{E})-\frac{1}{\rho d_\tau(\bar{E})}-\frac{1}{\lambda_\tau^{CC}(\bar{E})}\right)\right] \tag{12}$$

with $\bar{E}\equiv\bar{E}(X-T;E)$, and

$$G_\nu(E,X)=n_N\int_{y_{\min}}^{y_{\max}}\frac{dy}{1-y}F_\nu(E_y,X)\frac{d\sigma_{\nu_\tau N\to\tau Y}}{dy}(y,E_y). \tag{13}$$

It is easy to see that the factor $Z_\nu(E,X)$ enters into the expression for $F_\tau(E,X)$ through the function $G_\nu(E,X)$. Similarly, $Z_\nu(E,X)$ also depends on $F_\tau(E,X)$. It is possible to solve for $Z_\nu(E,X)$ and $F_\tau(E,X)$ simultaneously by the iteration method [18]. The details are given in Appendix B.

III. RESULTS AND DISCUSSION

In the following, we show the tau-lepton fluxes resulting from three kinds of diffuse astrophysical neutrino fluxes: the active galactic nuclei (AGN) [19], the gamma-ray burst (GRB) [20], and the GZK [21] neutrino fluxes. In these representative models, F_{ν_τ} arises because of neutrino flavor mixing [22]. The $p\gamma$ interactions are the source of intrinsic F_{ν_μ}, and $F_{\nu_\tau}=1/2\cdot F_{\nu_\mu}$ because of (two) neutrino flavor oscillations during propagation. Our convention for F_{ν_τ} is that $F_{\nu_\tau}=dN_{\nu_\tau}/d(\log_{10}E)$ in units of $\mathrm{cm}^{-2}\,\mathrm{s}^{-1}\,\mathrm{sr}^{-1}$. The same convention is used for the outgoing tau-lepton fluxes. For completeness, let us remark here that the recent upper bound on diffuse astrophysical F_{ν_μ} (not F_{ν_τ}) from the Antarctic Muon and Neutrino Detector Array (AMANDA) B10 is of the order of $\sim 8.4\times10^{-7}\,\mathrm{cm}^{-2}\,\mathrm{s}^{-1}\,\mathrm{sr}^{-1}\,\mathrm{GeV}$ for $6\times10^3\leqslant E_\nu/\mathrm{GeV}\leqslant10^6$ [23]. This 90% classical confidence upper bound is mainly for upward going ν_μ with E^{-2} energy spectrum and includes the systematic uncertainties. As far as the AMANDA B10 upper bound on F_{ν_μ} is concerned, all three of our representative neutrino flux models are clearly compatible with this upper bound within its energy range.

In Fig. 2, we show the outgoing tau-lepton energy spectra resulting from the propagation of incident AGN neutrinos inside rock ($\rho=2.65\ \mathrm{g/cm}^3$) for $X/\rho=10$ km, 100 km, and 500 km, respectively. It is interesting to see that the tau-lepton energy spectra remain almost unchanged for the above three different slant depth/matter density ratio values. This feature can be understood by two simple facts. First of all, the neutrino-nucleon charged-current interaction length, which is related to the interaction thickness by $\lambda_{CC}=\rho l_{CC}$, is given by $l_{CC}=2\times10^4\ \mathrm{km}\ [(1\ \mathrm{g/cm}^3/\rho)][E_\nu/(10^6\ \mathrm{GeV})]^{-0.363}$. Secondly, the tau leptons, which eventually exit the Earth, ought to be produced within a tau-lepton range distance to the exit point. For a tau-lepton produced far away from the exit point, it loses energy and decays before reaching the exit point. Hence the tau-lepton flux is primarily determined by the ratio of tau-lepton range to the charged-current neutrino-nucleon interaction length. The total slant depth X which the tau-neutrino (tau-lepton) traverses inside the Earth is then unimportant, unless X is large enough that the tau-neutrino flux attenuates significantly before the tau neutrino is converted into the tau lepton. We note that the typical energy for the AGN neutrinos, in which this flux peaks, is between 10^5 and 10^8 GeV. The corresponding neutrino-nucleon neutral-current interaction length then ranges from 42 000 km down to 3400 km, given $l_{\mathrm{NC}}=2.35\cdot l_{\mathrm{CC}}$. Hence, even for X/ρ as large as 500 km, the attenuation of the tau-neutrino flux is negligible. This explains the insensitivity of tau-lepton flux with respect to our chosen X/ρ values for the AGN case. The situation is rather similar for the tau-lepton flux resulting from the GRB tau neutrinos (see Fig. 3). On the other hand, a slight suppression is found for the GZK case at $E_\tau>10^9$ GeV as one increases X/ρ from 10 km to 500 km (see Fig. 4). This is because the typical GZK tau-neutrino flux peaks in the energy range between 10^7 and 10^{10} GeV, which corresponds to attenuation lengths ranging from 7800 km down to 640 km. One notices

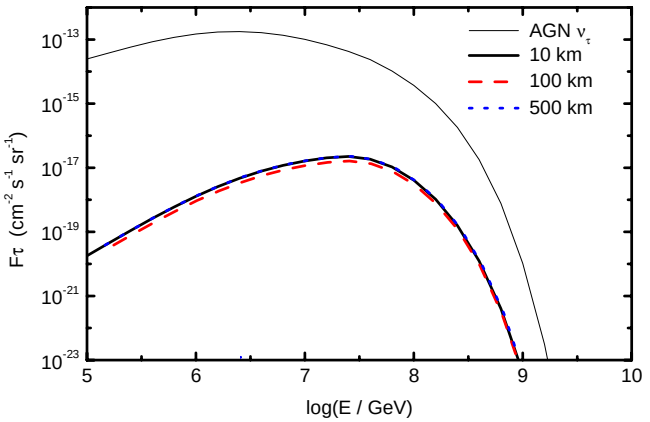

FIG. 2. The tau-lepton energy spectrum induced by the AGN neutrinos in rock for three different X/ρ ratio values (see text for more details). The incident tau-neutrino flux is shown by the thin solid line.

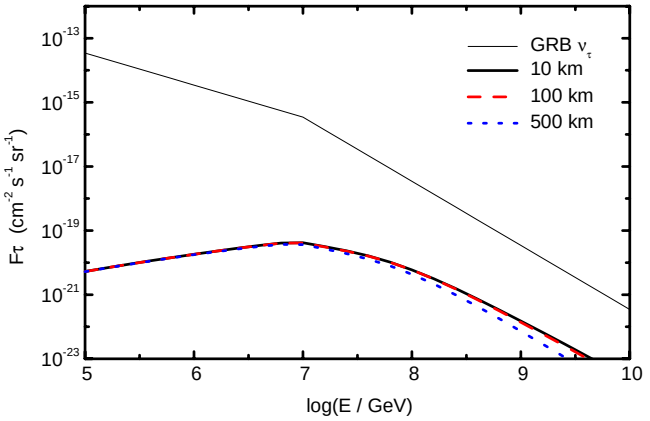

FIG. 3. The tau-lepton energy spectrum induced by the GRB neutrinos in rock for three different X/ρ ratio values (see text for more details). The incident tau-neutrino flux is shown by the thin solid line.

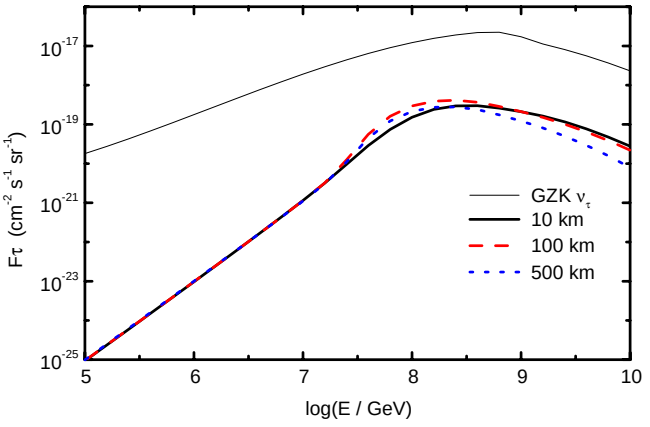

FIG. 4. The tau-lepton energy spectrum induced by the GZK neutrinos in rock for three different X/ρ ratio values (see text for more details). The incident tau-neutrino flux is shown by the thin solid line.

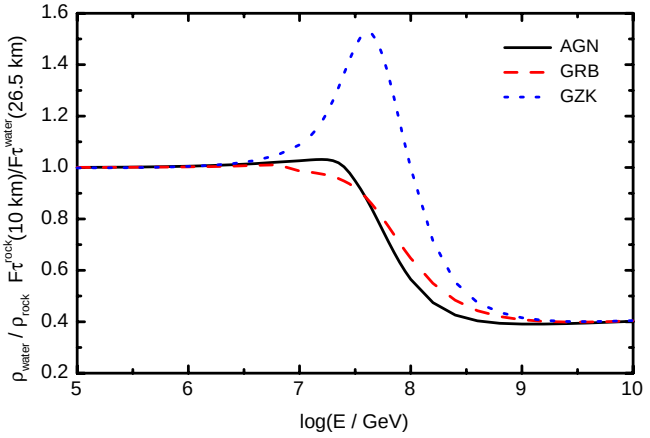

FIG. 5. The ratio of F_τ in rock and water induced by the AGN, the GRB, and the GZK neutrinos for $X=2.65\times10^6$ g/cm^2.

that 640 km is rather close to the distance 500 km which we choose for X/ρ. Hence a slight suppression in the tau-lepton flux occurs for $X/\rho=500$ km.

We have compared our AGN-type tau-lepton flux with that obtained by Monte Carlo simulations, adopting a stochastic approach for the tau-lepton energy loss [24]. The two tau-lepton fluxes agree within $\sim10\%$. This is expected since the tau-lepton ranges obtained by the above two approaches agree well, as pointed out before. It is easily seen from Figs. 2–4 that the AGN case has the largest tau-lepton flux between 10^6 and 10^8 GeV. Since the resonant $\bar{\nu}_e$-e^- scattering cross section peaks at $E_\nu=6.3\times10^6$ GeV, it is of interest to compare the integrated tau-lepton flux resulting from this scattering to the one arising from neutrino-nucleon scattering. For the former case, we integrate the tau-lepton energy spectrum from 10^6 GeV to 6.3×10^6 GeV, and obtain $\Phi_\nu^{\rm R}=0.08$ km^{-2} sr^{-1} yr^{-1}. For neutrino-nucleon scattering, we find that $\Phi_\nu^{\rm CC}=2.2$ km^{-2} sr^{-1} yr^{-1} by integrating the corresponding tau-lepton energy spectrum from 10^6 GeV to 10^7 GeV. The detailed results for $\Phi_\nu^{\rm CC}$ are summarized in Table I. The entries in the table entitled ''Full'' are obtained using the F_τ obtained in this work, whereas the approximated values entitled ''Approx'' are obtained by following the description given in Ref. [4], which uses a constant β and a constant inelasticity coefficient for $\nu_\tau N$ scattering. We remark that the authors of Ref. [4] have taken E to be greater than 10^8 GeV. Hence the integrated fluxes in the column ''Approx'' with energies less than 10^8 GeV are taken as extrapolations. Thus, one should compare the two integrated fluxes only for $E>10^8$ GeV. One can see that the two integrated fluxes seem to agree for $E>10^8$ GeV. In addition to the integrated fluxes for $E>10^8$ GeV, we also obtain integrated tau-lepton fluxes for $10^6\leqslant E/\text{GeV}\leqslant10^8$. It is easily seen that, in this energy range, the integrated tau-lepton flux from Earth-skimming AGN neutrinos is relatively significant.

It is possible that the tau-neutrino skims through a part of the ocean in addition to the Earth before exiting the interaction region [25]. Hence, it is desirable to compare the resulting tau-lepton fluxes as the tau neutrinos skim through media with different densities, while the slant depths of the media, are held fixed as an example. As stated before, the tau-lepton flux is essentially determined by the probability of $\nu_\tau N$ charged-current interaction happening within a tau-lepton range. Furthermore, from Fig. 1, it is clear that the tau-lepton range equals the tau-lepton decay length for E_τ less than 10^7 GeV. One therefore expects $F_\tau^{\rm rock}(E,X)/F_\tau^{\rm water}(E,X)=\rho^{\rm rock}/\rho^{\rm water}$ for $E_\tau<10^7$ GeV. This is clearly seen to be the case from Fig. 5 and Fig. 6, as we compare $F_\tau^{\rm rock}$ with $F_\tau^{\rm water}(E,X)$ for $X=2.65\times10^6$ g/cm^2 and $X=2.65\times10^7$ g/cm^2, respectively. For $E_\tau>10^7$ GeV, the tau-lepton range has additional dependencies on the mass density and the atomic number of the medium. Hence the ratio

TABLE I. Comparison of the integrated tau-lepton flux (km^{-2} yr^{-1} sr^{-1}) in different energy bins for the AGN, the GRB, and the GZK neutrinos without and with approximation (see text for details). The distance traversed is taken to be 10 km in rock here. For $10^9\leqslant E/\text{GeV}\leqslant10^{10}$, the incident AGN neutrino flux is too small so that its induced tau-lepton flux is not shown.

	AGN		GRB		GZK	
Energy interval	Full	Approx	Full	Approx	Full	Approx
$10^6\leqslant E/\text{GeV}\leqslant10^7$	2.23	2.12	9.63×10^{-3}	1.05×10^{-2}	7.38×10^{-5}	2.08×10^{-5}
$10^7\leqslant E/\text{GeV}\leqslant10^8$	4.89	5.12	7.12×10^{-3}	6.82×10^{-3}	1.14×10^{-2}	1.90×10^{-2}
$10^8\leqslant E/\text{GeV}\leqslant10^9$	1.95×10^{-1}	1.52×10^{-1}	5.39×10^{-4}	4.63×10^{-4}	8.17×10^{-2}	8.47×10^{-2}
$10^9\leqslant E/\text{GeV}\leqslant10^{10}$			1.13×10^{-5}	1.24×10^{-5}	3.31×10^{-2}	3.52×10^{-2}

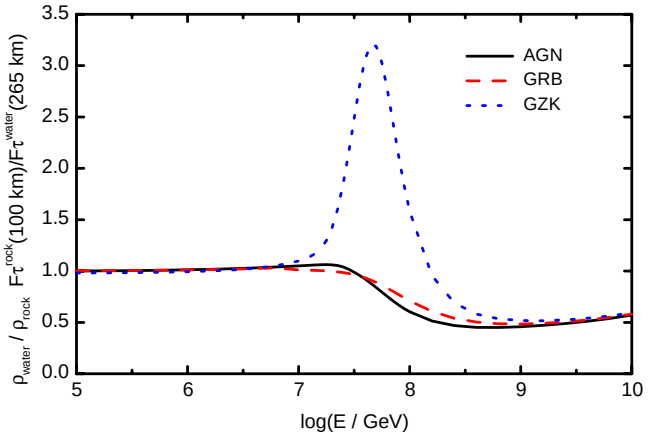

FIG. 6. The ratio of F_τ in rock and water induced by the AGN, the GRB, and the GZK neutrinos for $X=2.65\times10^7$ g/cm^2.

$F_\tau^{\rm rock}(E,X)/F_\tau^{\rm water}(E,X)$ starts deviating from $\rho^{\rm rock}/\rho^{\rm water}$. It is worthwhile to mention that the tau-lepton flux ratios for the AGN and GRB cases behave rather similarly. On the other hand, the ratio in the GZK case has a clear peak in the range $10^{7.5}<E/{\rm GeV}<10^{8.5}$. Such a peak is even more apparent for the slant depth $X=2.65\times10^7$ g/cm^2. The appearance of this peak has to do with the relatively flat behavior of the incident GZK neutrino spectrum, while the position of this peak is related to the energy dependencies of the tau-lepton range and the neutrino-nucleon scattering cross sections. We have confirmed our observations by computing the flux ratios with simple power-law incident tau-neutrino fluxes. The above peak in the tau-lepton flux ratio implies the suppression of tau-lepton events from ocean-skimming neutrinos compared to those from rock-skimming neutrinos. As stated earlier, the suppression of ocean-skimming neutrinos is related to the spectral index of the incident neutrino flux. It is therefore useful to perform a detailed simulation for it [26]. Such a detailed study is needed because the slant depths traversed by the above two kinds of neutrinos are generally different.

IV. PROSPECTS FOR POSSIBLE FUTURE OBSERVATIONS

To observe the above tau leptons, the acceptance of a detector must be of the order of $\sim$km^2 sr. For AGN neutrinos, the tau-lepton energy spectrum peaks at around 10^7–10^8 GeV, which is below the threshold of a fluorescence detector, such as the High Resolution Fly's Eye (HiRes) [27]. Also, these tau leptons come in near horizontally. At present, it seems very difficult to construct a ground array in the vertical direction. A Cherenkov telescope seems to be a feasible solution. In this context, the NuTel Collaboration is developing Cherenkov telescopes to detect the Earth-skimming high energy neutrinos [25]. However, because of the small opening angle of the Cherenkov light cone and only a 10% duty cycle (optical observations are limited to moonless and cloudless nights only), such a detector must cover a very large area and field of view. A potential site for NuTel is at Hawaii Big Island, where two large volcanos, namely, Mauna Loa and Mauna Kea, could be favorable candidates for high energy neutrinos to interact with. For a detector situated on top of Mount Hualalai and to look at both Mauna Kea and Mauna Loa, the required angular field of view is $\sim 8°\times120°$. Furthermore, this telescope should have an acceptance area larger than 2 km^2 sr so as to detect more than one event per year.

Concerning the GZK neutrinos, we note that the recent observation of ultrahigh energy cosmic rays by HiRes seem to be consistent with the GZK cutoff. Therefore a future observation of GZK tau neutrinos will provide a firm support to GZK cutoff. In particular, the slight pileup of tau leptons between 10^8 GeV and 10^9 GeV, induced by the Earth-skimming high energy GZK neutrinos, should be a candidate signature for GZK neutrinos. The integrated tau-lepton flux in this energy range is approximately 0.08 km^{-2} sr^{-1} yr^{-1}. To detect one event per year from this flux, the acceptance of a detector must be larger than 120 km^2 sr for a fluorescence detector (assuming a duty cycle of 10%). Although HiRes can reach 1000 km^2 sr at energy greater than 3×10^9 GeV, it would be a technical challenge to lower the threshold to 10^8 GeV. Using a system similar to HiRes, the Dual Imaging Cherenkov Experiment (DICE) was able to detect Cherenkov light from extensive air showers at energy as low as 10^5 GeV [28]. However, the field of view of DICE is also quite small, and thus several Cherenkov telescopes would be needed. An alternative method is a hybrid detection of both Cherenkov and fluorescence photons [29]. That is, a detector similar to HiRes, which looks at both land and sea and detects both Cherenkov and fluorescence photons, may observe the associated signal of GZK neutrinos.

In summary, we have given a semianalytic treatment of the problem of simultaneous propagation of high energy tau neutrinos and tau leptons inside the Earth. Our treatment explicitly takes into account the *inelasticity* of neutrino-nucleon scatterings as well as the tau-lepton *energy loss*. We specifically considered the Earth-skimming situation and provided detailed results for the energy dependencies of emerging tau-lepton fluxes resulting from a few anticipated astrophysical neutrino fluxes. The effect of matter density on the tau-lepton flux is also studied. Such an effect is found to be related to the spectrum index of the incident neutrino flux. Our treatment thus provides a basis for a more complete and realistic assessment of high energy neutrino flux measurements in the large neutrino telescopes under construction or being planned.

ACKNOWLEDGMENTS

We thank N. La Barbera for communicating his Monte Carlo–based results to us. H.A. thanks the Physics Division of NCTS for support. M.A.H. is supported by Taiwan's Ministry of Education under ''Research Excellence Project on Cosmology and Particle Astrophysics: Sub-project II'' with the grant number 92-N-FA01-1-4-2. F.F.L., G.L.L., J.J.T., and T.W.Y. are supported by the National Science Council of Taiwan under the grant numbers NSC91-2112-M009-019 and NSC91-2112-M-001-024.

APPENDIX A: THE CONTRIBUTION FROM RESONANT $\bar{\nu}_e e^-$ SCATTERING

The transport equations for $\bar{\nu}_e$ and the tau lepton are given by Eqs. (3) and (4). For convenience, let us write $1-y=z$. The last term in Eq. (4) can be simplified using

$$\frac{d\sigma^{-}_{\nu_e e^- \to \bar{\nu}_\tau \tau^-}}{dz}(z,E/z)=\frac{m_W^4 G_F^2}{\pi}\frac{s(1-z)^2}{(s-m_W^2)^2+m_W^2\Gamma_W^2} \tag{A1}$$

and the narrow width approximation

$$\frac{1}{\pi}\frac{m_W\Gamma_W}{(s-m_W^2)^2+m_W^2\Gamma_W^2}\approx\delta(s-m_W^2). \tag{A2}$$

We arrive at

$$\frac{\partial F_\tau(E,X)}{\partial X}=-\frac{F_\tau(E,X)}{\rho d_\tau(E)}+\frac{1}{3}\left(1-\frac{E}{E_R}\right)^2 \times\left(\frac{\pi\Gamma_W}{L_R m_W}\right)F^{-}_{\nu_e}(E_R,X), \tag{A3}$$

where $E_R=m_W^2/2m_e$ is the $\bar{\nu}_e$ energy such that the W boson is produced on shell in the $\bar{\nu}_e e^-$ scattering. $L_R \equiv 1/n_e\sigma^{-}_{\nu_e e^- \to W^-}$ is the interaction thickness for such a scattering. To solve for $F_\tau(E,X)$, we need to input $F^{-}_{\nu_e}(E_R,X)$. Obviously, the $\bar{\nu}_e$ flux at the resonant-scattering energy E_R is mainly attenuated by the resonant scattering itself. Hence $F^{-}_{\nu_e}(E_R,X)=\exp(-X/L_R)F^{-}_{\nu_e}(E_R,0)$. Substituting this result into Eq. (A3), we obtain

$$F_\tau(E,X)=\frac{1}{3}\left(1-\frac{E}{E_R}\right)^2\left(\frac{\pi\Gamma_W}{L_R m_W}\right)F^{-}_{\nu_e}(E_R,0) \times\exp\left(-\frac{X}{\rho d_\tau(E)}\right)\int_0^X dZ \times\exp\left[\left(\frac{1}{\rho d_\tau(E)}-\frac{1}{L_R}\right)Z\right]. \tag{A4}$$

The integration over Z can be easily performed. In practice, it is obvious that $X\gg\rho d_\tau(E)$. In this limit, we have

$$F_\tau(E,X)=\frac{\pi}{3}\left(1-\frac{E}{E_R}\right)^2\left(\frac{\Gamma_W}{m_W}\right)\left(\frac{\rho d_\tau(E)}{L_R}\right)F^{-}_{\nu_e}(E_R,0) \times\exp\left(-\frac{X}{L_R}\right). \tag{A5}$$

Let us consider standard rock as the medium for $\bar{\nu}_e e^-$ scattering; we then have $\rho/L_R=n_e\rho\sigma^{-}_{\nu_e e^- \to W^-}$. Given $\sigma^{-}_{\nu_e e^- \to W^-}=4.8\times10^{-31}$ cm^2 at the W boson mass peak, and $n_e\rho=2.65\times6.0/2\times10^{23}/\text{cm}^3$ in standard rock, we obtain $\rho/L_R=(26\text{ km})^{-1}$. Furthermore, we can write $d_\tau(E)=49\text{ km}\times(E/10^6\text{ GeV})$. We then obtain the following ratio:

$$\frac{F_\tau(E,X)}{F^{-}_{\nu_e}(E_R,0)}=3.3\times10^{-4}\times\left(\frac{E}{E_R}\right)\times\left(1-\frac{E}{E_R}\right)^2\times\exp\left(-\frac{X}{L_R}\right). \tag{A6}$$

This is the result given by Eq. (10) in the main text.

APPENDIX B: THE ITERATION METHOD FOR OBTAINING $Z_\nu(E,X)$ AND $F_\tau(E,X)$

The evolution for F_{ν_τ} is given by Eq. (1). With the ansatz

$$F_{\nu_\tau}(E,X)=F_{\nu_\tau}(E,0)\exp\left(-\frac{X}{\Lambda_\nu(E,X)}\right), \tag{B1}$$

we obtain the following equation for $Z_\nu(E,X)$:

$$XZ_\nu(E,X)=\int_0^X dX'\int_0^1\frac{dy}{1-y}\left\{\frac{F^{(0)}_{\nu_\tau}(E_y)}{F^{(0)}_{\nu_\tau}(E)}\exp[-X'D_\nu(E,E_y,X')]\Phi^{\text{NC}}_{\nu_\tau}(y,E) + \frac{F_\tau(E_y,X')}{F^{(0)}_{\nu_\tau}(E)}\left(\frac{\lambda_\nu(E)}{\rho d_\tau(E)}\right)\exp\left(\frac{X'}{\Lambda_\nu(E,X')}\right)\Phi^d_\tau(y,E)+\frac{F_\tau(E_y,X')}{F^{(0)}_{\nu_\tau}(E)}\left(\frac{\lambda_\nu(E)}{\lambda_\tau(E)}\right)\exp\left(\frac{X'}{\Lambda_\nu(E,X')}\right)\Phi^{\text{CC}}_\tau(y,E)\right\}, \tag{B2}$$

where $F^{(0)}_{\nu_\tau}(E) \equiv F_{\nu_\tau}(E,0)$, while $\Phi^{\rm NC}_{\nu_\tau}$, $\Phi^{\rm CC}_{\tau}$, and Φ^{d}_{τ} are respectively given by

$$\Phi^{\rm NC}_{\nu_\tau}(y,E) = \frac{\sum_T n_T (d\sigma_{\nu_\tau T \to \nu_\tau Y}/dy)(y,E_y)}{\sum_T n_T \sigma^{\rm tot}_{\nu_\tau T}(E)}, \tag{B3}$$

$$\Phi^{\rm CC}_{\tau}(y,E) = \frac{\sum_T n_T (d\sigma_{\tau T \to \nu_\tau Y}/dy)(y,E_y)}{\sum_T n_T \sigma^{\rm tot}_{\tau T}(E)}, \tag{B4}$$

$$\Phi^{d}_{\tau}(y,E) = \frac{1}{\Gamma_\tau(E)} \frac{d\Gamma_{\tau \to \nu_\tau Y}}{dy}(y,E_y), \tag{B5}$$

with n_T the number of targets per unit mass of the medium, and

$$D_\nu(E,E_y,X) = \frac{1}{\Lambda_\nu(E_y,X)} - \frac{1}{\Lambda_\nu(E,X)}. \tag{B6}$$

For simplicity in the notation, we take the lower and upper limits for the y integration to be 0 and 1, respectively. In reality, the limits depend on the actual kinematics of each process. One may impose these limits in the functions $\Phi^{\rm NC}_{\nu_\tau}$, $\Phi^{\rm CC}_{\tau}$, and Φ^{d}_{τ}.

To perform the iteration, we begin by setting $Z_{\nu(0)} = 0$. In this approximation, we have

$$F_{\nu_\tau(0)}(E,X) = F_{\nu_\tau}(E,0) \exp\left(- \frac{X}{\lambda_\nu(E,X)} \right). \tag{B7}$$

Substituting $F_{\nu_\tau(0)}(E,X)$ into Eq. (12), we obtain the lowest order ν_τ flux, $F_{\tau(0)}(E,X)$. The first iteration for Z_ν, denoted by $Z_{\nu(1)}$ is calculable from Eq. (B2) by substituting $F_{\nu_\tau(0)}(E,X)$, $F_{\tau(0)}(E,X)$, and $Z_{\nu(0)}$ into the RHS of this equation. From $Z_{\nu(1)}$, we can then calculate $F_{\nu_\tau(1)}(E,X)$ and $F_{\tau(1)}(E,X)$, which corresponds to the results presented in this paper. We have checked the convergence of the iteration procedure and have found negligible differences between $Z_{\nu(2)}$ and $Z_{\nu(1)}$ and their associated ν_τ and τ fluxes.

The value of Z_ν depends on the spectrum index of the neutrino flux, since it effectively gives the regeneration effect in the neutrino-nucleon scattering. In general, a flatter neutrino spectrum implies a larger Z_ν. Z_ν is, however, not sensitive to the slant depth X. In the case of GRB neutrinos, where the flux decreases as E_ν^{-2} for $E_\nu < 10^7$ GeV and decreases as E_ν^{-3} for energies greater than that, we obtain $Z_\nu^{\rm GRB} \approx 0.2$. For the AGN neutrino, $Z_\nu^{\rm AGN}$ changes from 0.96 to 0.35 as E_ν runs from 10^5 GeV to 10^6 GeV. In this energy range, the neutrino flux decreases more slowly than $E_\nu^{-0.5}$. For E_ν greater than 10^8 GeV, $Z_\nu^{\rm AGN}$ drops below 0.2 as the neutrino flux spectrum begins a steep fall. The values for $Z_\nu^{\rm GZK}$ also follow a similar pattern.

[1] S.W. Barwick, lectures presented at 28th SLAC Summer Institute on Particle Physics: Neutrinos from the Lab, the Sun, and the Cosmos (SSI 2000), Stanford, California, USA, 2000; H. Athar, hep-ph/0209130. For a recent review article, see H. Athar, hep-ph/0212387.

[2] G. Domokos and S. Kovesi-Domokos, hep-ph/9801362; hep-ph/9805221; see also D. Fargion, Astrophys. J. **570**, 909 (2002).

[3] X. Bertou, P. Billoir, O. Deligny, C. Lachaud, and A. Letessier-Selvon, Astropart. Phys. **17**, 183 (2002).

[4] J.L. Feng, P. Fisher, F. Wilczek, and T.M. Yu, Phys. Rev. Lett. **88**, 161102 (2002).

[5] S. Bottai and S. Giurgola, Astropart. Phys. **18**, 539 (2003).

[6] RICE Collaboration, I. Kravchenko *et al.*, astro-ph/0306408; see also, M. Chiba *et al.*, in *Radio Detection of High Energy Particles*, edited by D. Saltzberg and P. Gorham, AIP Conf. Proc. No. 579 (AIP, Melville, NY, 2001), p. 204.

[7] http://www.ps.uci.edu/~anita/

[8] L.V. Volkova, G.T. Zatsepin, and L.A. Kuzmichev, Yad. Fiz. **29**, 1252 (1979) [Sov. J. Nucl. Phys. **29**, 645 (1979)].

[9] S.L. Glashow, Phys. Rev. **118**, 316 (1960).

[10] For a recent discussion, see H. Athar and G.-L. Lin, Astropart. Phys. **19**, 569 (2003), and references cited therein.

[11] S. Iyer Dutta, M.H. Reno, I. Sarcevic, and D. Seckel, Phys. Rev. D **63**, 094020 (2001).

[12] B. Rossi, *High Energy Particles* (Prentice-Hall, Englewood Cliffs, NJ, 1952).

[13] A.A. Petrukhin and V.V. Shestakov, Can. J. Phys. **46**, S377 (1968).

[14] R.P. Kokoulin and A.A. Petrukhin, in Proceedings of the XII International Conference on Cosmic Rays, Hobart, Tasmania, Australia, 1971, Vol. 6.

[15] L.B. Bezrukov and E.V. Bugaev, Yad. Fiz. **33**, 1195 (1981) [Sov. J. Nucl. Phys. **33**, 635 (1981)]. For a recent discussion, see E.V. Bugaev and Y.V. Shlepin, Phys. Rev. D **67**, 034027 (2003).

[16] P. Lipari and T. Stanev, Phys. Rev. D **44**, 3543 (1991).

[17] J. Pumplin, D.R. Stump, J. Huston, H.L. Lai, P. Nadolsky, and W.K. Tung, J. High Energy Phys. **07**, 012 (2002).

[18] V.A. Naumov and L. Perrone, Astropart. Phys. **10**, 239 (1999).

[19] A. Neronov, D. Semikoz, F. Aharonian, and O. Kalashev, Phys. Rev. Lett. **89**, 051101 (2002); O.E. Kalashev, V.A. Kuzmin, D.V. Semikoz, and G. Sigl, Phys. Rev. D **66**, 063004 (2002).

[20] E. Waxman and J.N. Bahcall, Phys. Rev. Lett. **78**, 2292 (1997); Phys. Rev. D **59**, 023002 (1999).

[21] V.S. Berezinsky and G.T. Zatsepin, Phys. Lett. **28B**, 423 (1969). For a recent discussion, see R. Engel, D. Seckel, and T. Stanev, Phys. Rev. D **64**, 093010 (2001).

[22] H. Athar, Nucl. Phys. B (Proc. Suppl.) **122**, 305 (2003); H. Athar, K. Cheung, G.-L. Lin, and J.-J. Tseng, Astropart. Phys. **18**, 581 (2003).

[23] AMANDA Collaboration, J. Ahrens *et al.*, Phys. Rev. Lett. **90**, 251101 (2003).

[24] N. La Barbera (private communication).
[25] G.W. Hou and M.A. Huang, in *Proceedings of the 1st NCTS Workshop on Astroparticle Physics*, Taiwan, 2001, edited by H. Athar, G.-L. Lin, and K.-W. Ng (World Scientific, Singapore, 2002), pp. 105–116, astro-ph/0204145. See also http://hep1.phys.ntu.edu.tw/nutel/
[26] M.A. Huang, G.-L. Lin, and J.-J. Tseng (in progress).
[27] HiRes-MIA Collaboration, T. Abu-Zayyad *et al.*, Astrophys. J. **557**, 686 (2001).
[28] S.P. Swordy and D.B. Kieda, Astropart. Phys. **13**, 137 (2000).
[29] Z. Cao, M.A. Huang, P. Sokolsky, and R.W. Springer, in Proceedings of the 28th International Cosmic Ray Conference, Tsukuba, Japan, 2003 (in preparation).